# 小児の特徴と現場における小児用量の考え方

国立成育医療研究センター研究所社会・臨床研究センター　中村 秀文

調剤の現場では，通常は薬用量ハンドブックやガイドラインなどを参考に医薬品選択や用量の確認を行うことが多いであろう。本稿ではこれら資料を活用する際に知っておくと役に立つ小児の特徴や薬用量設定の基本的考え方について紹介する。小児における薬剤の選択と薬用量・投与間隔の設定を適切に行うためには，薬物動態学と薬力学の両方における特徴を理解しておく必要がある。吸収，分布，代謝，排泄に関わる薬物動態パラメータがわかれば，目標とする血中濃度を得るための投与量・投与間隔を決定することができる。推奨されている薬用量には，体重当たりの投与量が設定されているもの，年齢幅ごとの投与量が設定されているもの，体表面積当たりの投与量が設定されているものなどがあり，一律ではない。抗がん薬などを除いては，一般的に体重当たりあるいは年齢幅ごとの投与量設定が行われている。一方，古典的な小児薬用量の算出式は年齢，体重，体表面積などに基づいて一律に計算されるよう設定されているが，これらを用いても必ずしも適切な薬用量を算出できないことも多い。しかし，安全域が広く血中濃度がぶれても有効でさほど安全性に問題がない古くから使われている薬物については，このような換算による投与量がいまだに用いられている。

## 薬物動態学の基本概念

一般的に薬の投与量は，投与量・血中濃度と効果および副作用との関係を踏まえて決定されている。安全域が広い薬であればさほど投与量を気にする必要はないが，TDM（Therapeutic Drug Monitoring：治療的薬物モニタリング）が行われるような薬は，血中濃度が少し変わると副作用が出たり，効果に変化が出たりするため，血中濃度をモニターしながら，用量，併用薬，また場合によっては剤形などについても十分に配慮する必要がある。

薬物動態については，薬学部で複雑な数式を学んだ記憶があると思うが，本稿ではワンコンパートメントモデル（一次速度過程，図1）を用いて基本概念・パラメータについて説明を試みる。フェニトインのように代謝が有効血中濃度内で飽和するよ

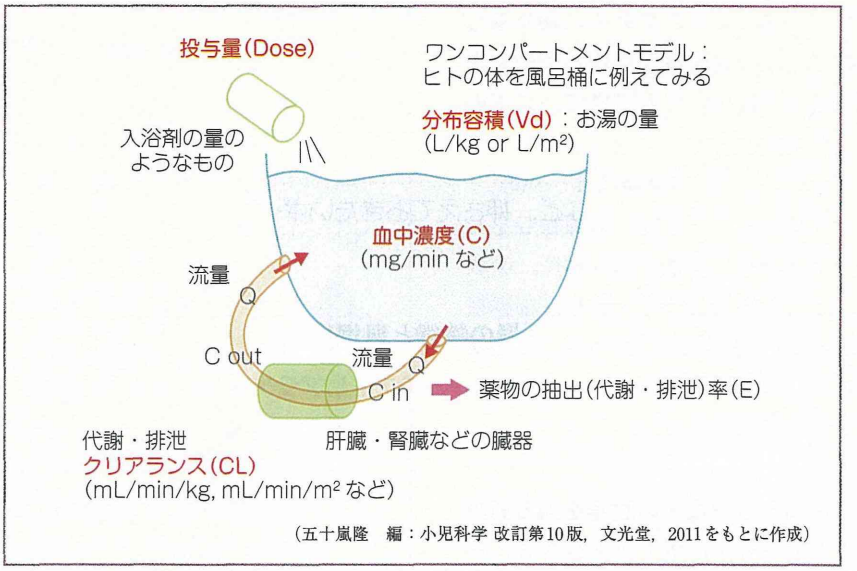


（五十嵐隆　編：小児科学 改訂第10版，文光堂，2011をもとに作成）

図1 薬物投与と薬物動態のワンコンパートメントモデルのイメージ

うな薬にはこのモデルは当てはまらないが，多くの場合にはこのモデルの考え方を理解していれば，薬物動態や用量設定についての基本的な考察を行うことができる。あくまで臨床的な理解のための説明であるので，よりくわしく学びたい場合は他の正書を参考にしていただきたい。

## 1. 分布容積

このモデルでは，体全体を血漿（血漿中濃度を測定する場合）や血清（血清中濃度を測定する場合）で構成されているかのように考える。体全体がどの程度の血漿もしくは血清量に相当するかの値を分布容積（volume of distribution）あるいは見かけの分布容積（apparent volume of distribution），略してVd（一般的には単位はL/kg，もしくはL/$m^2$で表す）と呼ぶ。

ヒトに薬（投与量D）を静脈内投与した場合にそれがすぐに体全体に分布すると仮定した場合，最高血中濃度C（0）は

$$C(0) = Dose/Vd \quad \cdots①$$

という投与量と分布容積だけの簡単な式で表すことができる。繰り返し投与の際の最大血中濃度と最低血中濃度の差についても同様で，以下の式で規定される。

$$C_{max} - C_{min} = Dose/Vd \quad \cdots②$$

ここでのポイントは，薬物投与をしたときの血中濃度の振れ幅は，吸収の要素を除けば“投与量と分布容積のみに規定される”ということである。

## 2. クリアランス

肝臓や腎臓などの臓器を通る薬のうちの一部が代謝・排泄される。その薬物排泄速度（rate of extraction もしくはrate of elimination）を血中濃度Cと関連づけるパラメーターとしてクリアランスが以下のように規定されている。

$$Rate\ of\ elimination = CL \cdot C \quad \cdots③$$

CLの単位は流量（小児では体重あるいは体表面積当たりで表示することが多い：mL/min/kg，mL/min/$m^2$など）であり，“生体または臓器が，ある単位時間に不可逆的に取り除く，薬を含んだ血液量”と定義される。

## 3. 半減期と定常状態

薬の半減期（$t_{1/2}$）は，投与された薬物血中濃度がある時点から2分の1の濃度になるまでに要する時間である。半減期は，以下の式によって，分布容積とクリアランスによって規定される。

$$t_{1/2} = 0.693 \cdot Vd/CL \quad \cdots④$$

臨床現場でよくある誤解は，“半減期＝薬の代謝・排泄能の指標”であるが，式④を見ればわかるように，これは間違いである。半減期の長い薬のクリアランスが必ずしも低いとは限らない。たとえクリアランスが高くてもその分布容積がより大きければ，半減期は長いこともある。

定常状態における持続点滴後の血中濃度Cssは，以下のように単純な式で表される。

$$Css = Rinf/CL \quad \cdots⑤$$

この式からわかるように，定常状態の血中濃度（繰り返し投与の際には平均血中濃度）は，投与速度（単位時間当たりの投与量）とクリアランスのみによって規定され，分布容積には規定されない。

臨床現場でその薬の現在の投与量が十分であるかどうかを評価する際には，投与を開始してどれくらい時間が経っているか，すなわち定常状態に達しているかを念頭に置いておかねばならないが，その評価には半減期が重要である。血中濃度は半減期の3倍で定常状態の約88%，半減期の5倍で定常状態の約97%に到達する。静注投与反復後の血中濃度推移と薬物動態パラメータの関係のイメージを図2に示す。

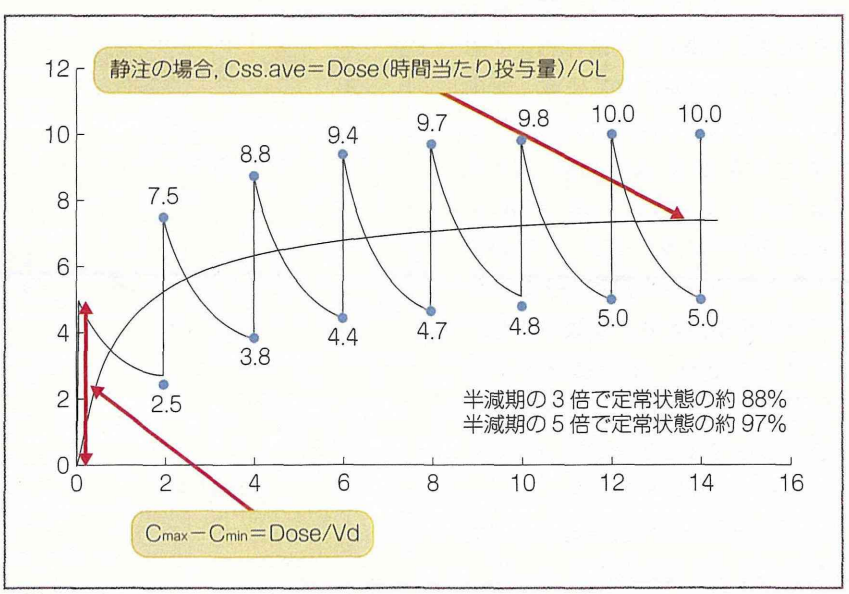


図2 **静脈内反復投与の際の薬物血中濃度推移と薬物動態パラメータの関係のイメージ**

## 4. 腎機能と薬物投与

治療域が狭く，腎臓から主に排泄される薬を投与している際，特にそれらに腎毒性がある場合（アミノグリコシド系抗菌薬やバンコマイシンなど）には，腎機能の指標として，血清クレアチニン（Cr）値などを，定期的に評価するべきである。Cr値は，薬の血中濃度と同じように，体内での生成と，分布容積，排泄のバランスによって決まっている。例えば60歳で70kgの成人のクレアチニンクリアランス（$CC_r$）は4.5L/hrであり，42Lの水分中に均等に分布しているから，式④を用いて，クレアチニンの半減期は，

$t_{1/2} = 0.693 \cdot 42\ (L)/4.5\ (L/hr)$
$= 6.5hr$

となる。クレアチニンの産生量，分布容積，クリアランスに変化がない状態（正常の状態もしくは慢性腎不全の状態）では，Cr値は定常状態に達しているために，測定されたCr値は，その時の腎機能を反映した値になっている。しかし，急激に腎機能が変化している状況では，Cr値は少なくともその1日以上前の腎機能を反映しており，測定時点での腎機能の指標にはなり得ない。

急激に腎機能が変化している場合，抗がん薬などで血中濃度時間曲線下面積（AUC）が副作用と効果に影響する薬では，初回投与量から減量を考慮せねばならないが，抗菌薬などの初回薬物投与は腎機能にかかわらず「通常投与量と同じでよい」ことが多い。なぜなら，式①にあるように，初回投与量は，分布容積と目標血中濃度から決定することができ，クリアランスの影響を受けないからである。一方，半減期は薬のクリアランスが落ちていることにより延長する。このため治療域が狭い医薬品では，2回目以降の投与量については適宜血中濃度の測定も考慮し調節する必要がある。その他の安全域が広い薬では，推定$CC_r$に応じた，大まかな減量規定が添付文書などに明示されているものもある。

血清クレアチニン値の正常値は，表1のように年齢によって異なり，成人における正常値であっても，小児では異常値となり得ることも知っておかなければならない。クレアチニン値以外にも発達に応じて正常値が変化するものもある。施設基準値としては成人値しか示されていない

表1 小児の血清クレアチニン値

測定法：酵素法　単位：mg/dL

| CRE男 | 下限値 | 中央値 | 上限値 |
|---|---|---|---|
| 0カ月 | 0.16 | 0.22 | 0.32 |
| 1カ月 | 0.15 | 0.21 | 0.31 |
| 2カ月 | 0.14 | 0.21 | 0.30 |
| 3カ月 | 0.14 | 0.20 | 0.30 |
| 4カ月 | 0.14 | 0.20 | 0.30 |
| 5カ月 | 0.14 | 0.20 | 0.30 |
| 6カ月 | 0.14 | 0.21 | 0.30 |
| 7カ月 | 0.14 | 0.21 | 0.30 |
| 8カ月 | 0.14 | 0.21 | 0.30 |
| 9カ月 | 0.15 | 0.22 | 0.31 |
| 10カ月 | 0.15 | 0.22 | 0.31 |
| 11カ月 | 0.16 | 0.23 | 0.32 |
| 1歳 | 0.16 | 0.24 | 0.33 |
| 7歳 | 0.27 | 0.40 | 0.53 |
| 15歳 | 0.42 | 0.68 | 0.95 |
| 20歳 | 0.50 | 0.80 | 1.00 |

| CRE女 | 下限値 | 中央値 | 上限値 |
|---|---|---|---|
| 0カ月 | 0.16 | 0.22 | 0.32 |
| 1カ月 | 0.15 | 0.21 | 0.31 |
| 2カ月 | 0.14 | 0.21 | 0.30 |
| 3カ月 | 0.14 | 0.20 | 0.30 |
| 4カ月 | 0.14 | 0.20 | 0.30 |
| 5カ月 | 0.14 | 0.20 | 0.30 |
| 6カ月 | 0.14 | 0.21 | 0.30 |
| 7カ月 | 0.14 | 0.21 | 0.30 |
| 8カ月 | 0.14 | 0.21 | 0.30 |
| 9カ月 | 0.15 | 0.22 | 0.31 |
| 10カ月 | 0.15 | 0.22 | 0.31 |
| 11カ月 | 0.16 | 0.23 | 0.32 |
| 1歳 | 0.16 | 0.24 | 0.33 |
| 7歳 | 0.25 | 0.38 | 0.51 |
| 15歳 | 0.35 | 0.55 | 0.75 |
| 20歳 | 0.35 | 0.55 | 0.75 |

（田中敏章　編：新しい小児の臨床検査基準値ポケットガイド，じほう，p38，2009をもとに作成）

場合が多いが，留意が必要である。

## 小児における薬物動態の特徴

### 1．薬の吸収

小児期の最も一般的な薬物投与法は経口投与である。胃内pHは，出生後すぐは6～8であるがその後数時間で1.5～3.0まで下がるとされている。その後，新生児期には比較的高いという報告と，低いままであるという報告がある。胃内容排出時間や腸管のぜん動，腸管粘膜の未熟性，薬物代謝酵素の未熟性などが，$T_{max}$や生体内利用率に影響する可能性も十分にある。一般的には，新生児・低出生体重児において薬の$T_{max}$は延長する。

経直腸投与後，上部直腸から吸収された薬は門脈に入るが，中部および下部直腸からは薬は門脈を経由せずに直接下大静脈に入り全身に分布する。したがって，直腸に投与され吸収された薬の多くは肝臓を通らず，初回通過効果を受けずに全身に分布することになる。生後2週から11歳の小児にジアゼパムを直腸内投与した後の血中濃度の上昇は，静脈内投与と変わらず，$T_{max}$は6分程度と報告されている。小児の痙攣重積治療にジアゼパム坐薬が有効とされるのはこのためである。しかし，坐薬の投与後すぐに排便があると，薬が排出される可能性があるために注意が必要である。また基剤の関係で，アセトアミノフェン坐薬と一緒に投与するとジアゼパムの吸収が遅れるとの報告があるため，両坐薬を同時に投与することは避けた方が良さそうである。ジアゼパムの効果をすぐに必要とする場合には，まずジアゼパム坐薬を投与し，20～30分待ってからアセトアミノフェン坐薬を投与する方がよいであろう。

### 2．薬の分布

薬の分布は，蛋白結合率，分子量，脂溶性／水溶性の程度，水分率や脂肪の量，体液のpH，それぞれの臓器・組織への血流の程度などのさまざまな因子に影響を受ける。通常新生児期には，水分率が高く，体脂肪量・筋肉量は少ない。例えば体重当たりの水分率は正期産児では約75%と，成人の50～60%よりもかなり高い。このため，水溶性の薬の中には，ゲンタマイシンなどのように，新生児などで分布容積が大きくなり，体重当たりの1回投与量が高めに設定されているものもある。

新生児は生理的に血中アルブミン濃度が低い。このために，アルブミンとの蛋白結合率の高いフェニトインのような医薬品では，血中濃度の評価に注意を要する。すなわち，低アルブミン血症では，フェニトインの総血中濃度は下がるけれども，遊離の血中濃度は，血中アルブミン濃度が正常な場合とさほど変わらないことも多い。薬の中には内因性物質と蛋白結合を競合し，内因性物質の分布に影響するものもある。特に新生児で問題となるのは，ビリルビンとアルブミン結合を競合する薬剤で，そのような薬の多くは，遊離したビリルビンにより核黄疸を起こす可能性があるために，新生児期での投与は禁忌とされている（例：スルファメトキサゾール）。

### 3．薬の代謝・排泄

#### (1) 薬物代謝の発達による変化

薬物代謝酵素活性は成熟に伴い変化することが知られている。成人の肝臓で最も豊富に存在するシトクロームP450（CYP）であるCYP3A4は胎児の肝臓にはほとんどなく，CYP3A7が主なCYP3Aである。CYP3A7は生後すぐをピークにその後急速に消失し，一方CYP3A4は生後1週間以内に出現し急速に増えていく。CYP2C9，CYP2C19，CYP2D6，CYP2E1なども出生後数日～数週でその活性が急速に上がるとされている。一方，発達による活性の上昇に，やや時間がかかるものもあり，CYP1A2の活性は，生後1～3カ月程度で初めて上昇を始める。

薬物代謝酵素の未熟性が副作用に関係するとされる良い例が，クロラムフェニコールによる灰白症候群（典型的には，成人通常量より高い100mg/kg/日以上を3～4日以上投与した新生児で，腹部膨満，嘔吐，皮膚蒼白，循環虚脱，呼吸停止などを起こす）である。一方，カルバマゼピンなどでは，体重当たりのクリアランスがむしろ小児の特定の年齢群で成人より高く，このような年齢群では1日投与量（体重当たり）が成人より高くなる。

#### (2) 薬物排泄の発達による変化

胎児における腎臓の形成は，在胎36週にはほぼ完了する。とは言え，生後しばらくは腎機能は未熟であり，出生後の日齢の増加にともない次第に心拍出量が増加し，また末梢血管抵抗が減少するために，腎血流量は増加する。早期産児では糸球体濾過率（GFR）は低く，0.6～0.8mL/min/1.73m$^2$程度のこともあるが，満期産児では2～4mL/min/1.73m$^2$であり，出生後2週間程度に急速に増加し，出生後8～12カ月くらいまでに，成人の値に近づくとされる。同

様に，尿細管分泌能も生後12カ月までに成人値に近づくとされている。腎排泄される薬の薬物動態はこの影響を受ける。例えば，ゲンタマイシンでは，1,000g未満の超低出生体重児では，腎機能の未熟さ（クリアランスが低い）と細胞外液量の多さ（分布容積が大きい）のために，推奨投与量は3.5mg/kgと多いが，半減期は長く24時間おき投与とされている。

## 小児における薬力学と特有の副作用

薬物動態に比べると，薬力学の発達による変化についてはまだ不明な点が多く，最近ようやく研究が進み始めたところである。シクロスポリンについては，末梢血単球によるIL-2産生抑制の$IC_{90}$と，末梢血単球増殖抑制の$IC_{50}$ともに，小児では成人と比べ低いという報告がある。小児の急性リンパ性白血病については治療の有効性や予後と関係する多くの遺伝子変異がわかっている。ワルファリンの治療効果には，成人と小児で差があることがかねてより報告されている。

医薬品には添加剤が含まれているものが多く，ものによっては成人では安全と考えられているが，新生児には副作用を起こすものもある。例えば注射薬に殺菌剤として添加されているベンジルアルコールは，新生児における代謝が遅いために蓄積し，あえぎ症候群（脳室内出血，代謝性アシドーシスなどを起こし重篤な場合には死亡する）を起こすことが知られており，現在では新生児に対して用いるべきではないとされている。また，溶解補助剤のプロピレングリコールも未熟児において蓄積することにより高浸透圧血症を起こし，呼吸循環不全や痙攣を起こすことが知られており，可能な限り避けた方がよいと考えられている。小児における薬の副作用についての機序解明も進みつつある。バルプロ酸の肝障害は，0～2歳の多剤併用療法患者でその頻度が約500分の1と高いことが知られているが，これは薬物代謝の発達による違いが一因であると考えられている。

その他の小児に特有とされる副作用には，テトラサイクリン系抗菌薬による歯牙の着色・エナメル質形成不全，デスフルランによる喉頭攣縮や分泌過多，ベラパミルによる乳児死亡などがある。今後，さらなる発症機序の解明が進むことを期待したい。

## 薬用量ハンドブック，ガイドラインと薬物投与

診療ガイドラインや治療ガイドラインを作成する際には，最近では「Minds診療ガイドライン作成の手引き2007」などに基づき，エビデンスをもとに，一定の手順に則って作成されているものが多く，エビデンスのレベル分類や推奨グレードが併記されているものも多い。

ガイドラインを作成する際には，まず医療者が臨床現場で直面する疑問をクリニカル・クエスチョンとして提示し，これに対するエビデンス検索を行い，答えの形で推奨文を作成する。このクリニカル・クエスチョン作成方法の1つとして以下のようなPICO形式を用いる方法がある。

P：patient，population，problem（どのような対象に）

I（E）：intervention，indicator，exposure（どのような治療を行ったら）

C：comparison，control（治療を行わない場合に比べて）

O：outcome（どれだけ結果が違うか）

臨床現場における治療の決定の際にもこのPICO形式を用いて治療を考えることができる。ガイドラインを参考にする際には常に臨床試験の対象集団と実際に目の前で治療をしようとしている患者との違いや，治療目的等の違いなどにも配慮しておかなければならない。

感染症に対する抗菌薬の投与量と投与期間は，臨床試験によってきちんとその有効性が評価されて定められていることが多い。このような場合，投与回数，投与期間などを勝手に変えては，期待された効果が得られず，また耐性菌の発現につながる可能性がある。一方，臨床効果を見ながら，投与量・投与間隔を変えるべき薬もある。アセトアミノフェンの解熱・鎮痛効果は4～6時間程度しか持続しないため，効果の持続を期待する場合は4～6時間間隔の投与が必要になる。ただし，本人が熱や痛みで苦しんでいる場合はともかく，高熱でもピンピンしていたり眠っている場合などには，投与する必要はない。解熱・鎮痛が目的であり，背景疾患の治癒が目的ではないからである。一方，10mg/kgの投与量で熱の下がりが悪くぐずる場合などは，間隔が2～3時間でももう10mg/kg投与する，あるいは1回15mg/kgを投与しても構わない。消耗がさほどない通常の小児で，併用注意薬などの投与がなければ，1日総量が概ね60mg/kgを越えなけれ

ば，投与間隔が短い，あるいは1回の投与量が少々多くなっても構わない。子どもが痛みや熱でつらそうな場合，それをいったん和らげてあげると，その間に食事が取れたり，眠ってしまったりすることも多い。一律に“38.5度以上で投与”などと指導するのは必ずしも適切ではない。

小児科領域における薬物治療の問題点として，①十分な症例数のランダム化比較試験などによる評価が行われていないものが多い，②希少疾病においては診断基準や有効性の評価基準も成人のように確立していないものも多い，③臨床試験間で評価指標が必ずしも統一されておらず評価目的も異なる――などが挙げられる。このような理由もあり，ガイドライン上でもエビデンスレベルや推奨グレードがさほど高くない治療も多く見られる。薬剤師としての知識も活用して，他の文献などにも可能な限り目を通し，個々の患者に最適な治療を考えていくことができるとすばらしい。

薬物投与を行う際には，その目的，期待する効果，留意すべき副作用などについて理解し，またどのように効果を判定し，それを踏まえてどの時点で中止すべきかなどもあらかじめ計画したうえで，開始するべきである。ただ漫然と治療を続けたり，薬の数を増やしていくことは，薬剤経済学的な観点からも副作用防止の観点からも避けなければならない。

小児用量が確立されていない薬については，国内外の文献を詳細に検討し有効性や安全性についての推測を可能な限り行い，開始用量については，体重や体表面積で換算した用量などとも比較したうえで，決定することになる。最近では，成人や他の疾患でも薬物動態や生理学的情報などを考慮した薬物動態と薬力学のモデリングも行われるようになっており，将来的には臨床現場でも活用されるようになることが期待される。このような試験的治療は，有効性の評価をどのように行うか，どのような副作用に気をつけるべきであるか，投与量をどのように増量・減量・中止するかなどを決めてから，開始するべきである。また数例で治療効果が認められると判断された場合には，いたずらに症例を重ねるのではなく，できるだけ早期に臨床試験を計画・実施し，用量設定や有効性・安全性の評価をより科学的に行うことが好ましい。医薬品の評価を適切に行おうとすること，またできるだけ早期に臨床試験を実施することが，小児薬物治療の質の向上につながることを忘れてはならない。

**参考文献**


1) 五十嵐隆　編：小児科学改訂第10版，文光堂，2011
2) 田中敏章　編：新しい小児の臨床検査基準値ポケットガイド，じほう，2009
3) Rowland M, et al.: Clinical pharmacokinetics and pharmacodynamics. Concepts and applications, 4th ed, Lippincott Williams & Wilkins, 2009
4) Jacqz-Aigrain E, Choonara I: Paediatric Clinical Pharmacology, Fontis Media, Lausanne and Taylor & Francis Group, 2006
5) Yaffe SJ, Aranda JV: Neonatal and pediatric pharmacology. Therapeutic principles in practice. 4th ed. Lippincot Williams & Wilkins, 2010
6) Kearns GL, et al.: Developmental pharmacology-Drug disposition, action, and therapy in infants and children. N Engl J Med, 349 (12): 1157-1167, 2003

OPEN ACCESS Freely available online

PLOS | ONE

# DNA Methylation Profile Distinguishes Clear Cell Sarcoma of the Kidney from Other Pediatric Renal Tumors

**Hitomi Ueno[1], Hajime Okita[1]*, Shingo Akimoto[1], Kenichiro Kobayashi[1], Kazuhiko Nakabayashi[2], Kenichiro Hata[2], Junichiro Fujimoto[3], Jun-ichi Hata[4], Masahiro Fukuzawa[5], Nobutaka Kiyokawa[1]**

**1** Department of Pediatric Hematology and Oncology Research, National Research Institute for Child Health and Development, Setagaya-ku, Tokyo, Japan, **2** Department of Maternal-Fetal Biology, National Research Institute for Child Health and Development, Setagaya-ku, Tokyo, Japan, **3** Director of Clinical Research Center, National Center for Child Health and Development, Setagaya-ku, Tokyo, Japan, **4** College of Human Science, Tokiwa University, Mito, Ibaraki, Japan, **5** President of Osaka Medical Center and Research Institute for Maternal and Child Health, Osaka Medical Center and Research Institute for Maternal and Child Health, Izumi, Osaka, Japan

## Abstract

A number of specific, distinct neoplastic entities occur in the pediatric kidney, including Wilms' tumor, clear cell sarcoma of the kidney (CCSK), congenital mesoblastic nephroma (CMN), rhabdoid tumor of the kidney (RTK), and the Ewing's sarcoma family of tumors (ESFT). By employing DNA methylation profiling using Illumina Infinium HumanMethylation27, we analyzed the epigenetic characteristics of the sarcomas including CCSK, RTK, and ESFT in comparison with those of the non-neoplastic kidney (NK), and these tumors exhibited distinct DNA methylation profiles in a tumor-type-specific manner. CCSK is the most frequently hypermethylated, but least frequently hypomethylated, at CpG sites among these sarcomas, and exhibited 490 hypermethylated and 46 hypomethylated CpG sites in compared with NK. We further validated the results by MassARRAY, and revealed that a combination of four genes was sufficient for the DNA methylation profile-based differentiation of these tumors by clustering analysis. Furthermore, *THBS1* CpG sites were found to be specifically hypermethylated in CCSK and, thus, the DNA methylation status of these *THBS1* sites alone was sufficient for the distinction of CCSK from other pediatric renal tumors, including Wilms' tumor and CMN. Moreover, combined bisulfite restriction analysis could be applied for the detection of hypermethylation of a *THBS1* CpG site. Besides the biological significance in the pathogenesis, the DNA methylation profile should be useful for the differential diagnosis of pediatric renal tumors.

**Citation:** Ueno H, Okita H, Akimoto S, Kobayashi K, Nakabayashi K, et al. (2013) DNA Methylation Profile Distinguishes Clear Cell Sarcoma of the Kidney from Other Pediatric Renal Tumors. PLoS ONE 8(4): e62233. doi:10.1371/journal.pone.0062233

**Editor:** Qian Tao, The Chinese University of Hong Kong, Hong Kong

**Received** December 25, 2012; **Accepted** March 19, 2013; **Published** April 26, 2013



**Funding:** This work was supported by Health and Labour Sciences Research Grants (the 3rd-term comprehensive 10-year strategy for cancer control H22-011), Grant-in-Aid for Scientific Research (B)(23390405, Grant of National Center for Child Health and Development (22A-5, 24-4), and Program for Promotion of Fundamental Studies in Health Sciences of the National Institute of Biomedical Innovation (NIBIO, 10-41, -42, -43, -44, -45). The funders had no role in the study design, data collection and analysis, decision to publish, or preparation of the manuscript.

**Competing Interests:** The authors have declared that no competing interests exist.

* E-mail: okita-h@ncchd.go.jp

## Introduction

In the pediatric population, the types of renal tumor are entirely different from those occurring in adults. It is estimated that 85% of pediatric renal malignancies comprise nephroblastoma, 5% congenital mesoblastic nephroma (CMN), 4% clear cell sarcoma of the kidney (CCSK), and 2% rhabdoid tumor of the kidney (RTK) [1], and these 4 major entities account for 96% of the total. The remaining 4% tend to occur in older children and include miscellaneous tumors, such as the Ewing's sarcoma family of tumors (ESFT). Nephroblastoma is malignant but still a relatively favorable tumor prognostically, being derived from nephrogenic blastemal cells that can show divergent differentiation. CMN is a kind of fibroblastic sarcoma of infancy and characterized by a specific chromosomal translocation, t(12;15)(p13;q25), which results in the fusion of *ETV6* and *NTRK3* genes [2]. On the other hand, CCSK is a relatively unfavorable tumor prognostically, being composed of clear mesenchymal cells with a characteristic vascular pattern [3]. RTK is a highly aggressive tumor occurring in young children, has a dismal outcome, and is characterized by pathological rhabdoid features and molecular biallelic inactivation of the *SMARCB1* (*hSNF5/INI1*) gene [4–6].

Since pediatric renal tumors are diverse neoplastic entities, as described above, and require different therapeutic strategies, rapid and accurate diagnosis is crucial for adequate treatment. However, all those tumors are composed of small-to-medium-sized, round, oval, or spindle-shaped undifferentiated or immature cells, and often deceptively mimic each other, making the diagnosis difficult [7]. In RTK and CMN, molecular markers, i.e., loss of SMARCB1 expression and *ETV6-NTRK3* fusion, respectively, are useful for an ancillary diagnosis, whereas the diagnosis of nephroblastoma and CCSK is exclusively based on histologic features. Although numerous studies have been done, immunohistochemical features or recurrent genetic changes that can reliably distinguish CCSKs from other pediatric renal tumors have not identified [3,8]. Therefore, the identification of molecular signatures that can distinguish CCSK from other renal tumors should be useful and provide diagnostic confidence and accuracy.

Alterations of DNA methylation have been well documented as an important peculiarity of cancer cells [9,10], and two patterns of

DNA-methylation changes have been observed in cancer [11,12]. One is a global hypomethylation associated with increased chromosomal instability, the reactivation of transposable elements, and loss of imprinting. The other is hypermethylation of CpG islands located in promoter regions of tumor suppressor genes that has conventionally been associated with transcriptional silencing in cancer. These aberrant DNA methylations are thought to be closely related to the development of cancer. Therefore, the identification of specific DNA methylation markers would be helpful for understanding the pathogenetic mechanism as well as for developing new therapeutic strategies. In Wilms' tumor, hypermethylation of *HACE1*, *RASSF1A* and *SIM1* and hypomethylation of *GRIPR* were reported [13–16], whereas the DNA methylation analysis in pediatric renal sarcomas including RTK, CCSK has not been reported yet.

In an attempt to investigate the characteristics of DNA methylation of pediatric sarcomas including CCSK, RTK, and ESFT, we performed DNA methylation analysis using Illumina Infinium HumanMethylation27. In this paper, we demonstrated that each sarcoma had a distinct DNA methylation profile and could be classified by the methylation pattern of a set of specific genes. We further proposed a convenient assay for the differential diagnosis of CCSK from other pediatric renal tumor.

## Materials and Methods

### Ethics Statement

This study was approved by the ethics committee/IRB at the National Center for Child Health and Development, and written informed consent was obtained from parents for samples from JWiTS. Since written informed consent was not obtained in a subset of samples collected before 2001, the identifying information for them was removed before analysis, in accordance with the Ethical Guideline for Clinical Research enacted by the Japanese Government. The ethics committee/IRB approved the waiver of written informed consent for latter samples.

**Table 2.** The number of hyper- and hypomethylated genes in comparison with non-neoplastic kidney.

| | CpG island probe | |
|---|---|---|
| | **Hypermethylated** | **Hypomethylated** |
| CCSK | 490 probes (437 genes) | 46 probes (36 genes) |
| RTK | 130 probes (107 genes) | 65 probes (62 genes) |
| ESFT | 66 probes (58 genes) | 55 probes (46 genes) |
| | **Non-CpG island probe** | |
| | **Hypermethylated** | **Hypomethylated** |
| CCSK | 184 probes (166 genes) | 117probes (112 genes) |
| RTK | 179 probes (160 genes) | 320probes (275 genes) |
| ESFT | 113 probes (101 genes) | 136probes (124 genes) |

Hypermethylation: difference of average β-value >0.3. Hypomethylation: difference of average β-value<−0.3.
doi:10.1371/journal.pone.0062233.t002

### Clinical Materials

Clinical specimens from pediatric patients, including 6 each with RTK and Ewing's sarcoma, 21 with CCSK, 9 with CMN, and 41 with Wilms' tumor, used in this study were selected from the files of specimens collected in our laboratory between 1985 and 2001, and the JWiTS (Japan Wilms Tumor Study). In each case, the pathological diagnosis was confirmed by J.H. and H.O. based on morphological observations and the immunophenotypic characteristics. Three non-neoplastic kidney (NK) tissues were obtained from the non-tumorous part of the above specimens.

### Sample Preparation

Each disease tissue was evaluated by preparing frozen section and the neoplastic cells accounted for more than 80% of viable

**Table 1.** Primers used for MassARRAY.

| Primer name | 5′ - 3′ sequence |
|---|---|
| ADRA1D_F | aggaagagagTGGTAGGTAATTTGTTTGTTATTTTTTT |
| ADRA1D_R | cagtaatacgactcactatagggagaaggctCTTCCAACCCAACAAAAACCCTA |
| ALDOC_F | aggaagagagTTGAATTTGGGTATTTTGAAGATGT |
| ALDOC_R | cagtaatacgactcactatagggagaaggctCAAATAAAACTACAACCCTAACTCCC |
| CREG1_F | aggaagagagGTGAGTAATTTGTAGGTGAGTTGGG |
| CREG1_R | cagtaatacgactcactatagggagaaggctCCACTACACTCCAACCTAAACCA |
| MGMT_F | aggaagagagTGAGATTGTTAGAGTGTGTTTTTGG |
| MGMT_R | cagtaatacgactcactatagggagaaggctTCCACTCAAACCAACTAAATTACCTA |
| PKN1_F | aggaagagagGGTTTTTTTTGGAGAATTAGAAGGG |
| PKN1_R | cagtaatacgactcactatagggagaaggctCCAACCACCATACAAAAAAATAAAA |
| PTEN_F | aggaagagagGGGGTTGTAAATAGATTTGATAGGTT |
| PTEN_R | cagtaatacgactcactatagggagaaggctAAAAAAAATCCCCAAACTAATACCA |
| THBS1_F | aggaagagagGGAGAGAGGAGTTTAGATTGGTTTT |
| THBS1_R | cagtaatacgactcactatagggagaaggctACCTTACCCTAAAAAATCCTCCAAC |
| VHL_F | aggaagagagTTTTGGGGAGATTGATAGATGTAAA |
| VHL_R | cagtaatacgactcactatagggagaaggctAACCACTTAACCCCAAATAACAAAT |

F, forward; R, reverse. Lower case letters indicate tag sequences.
doi:10.1371/journal.pone.0062233.t001

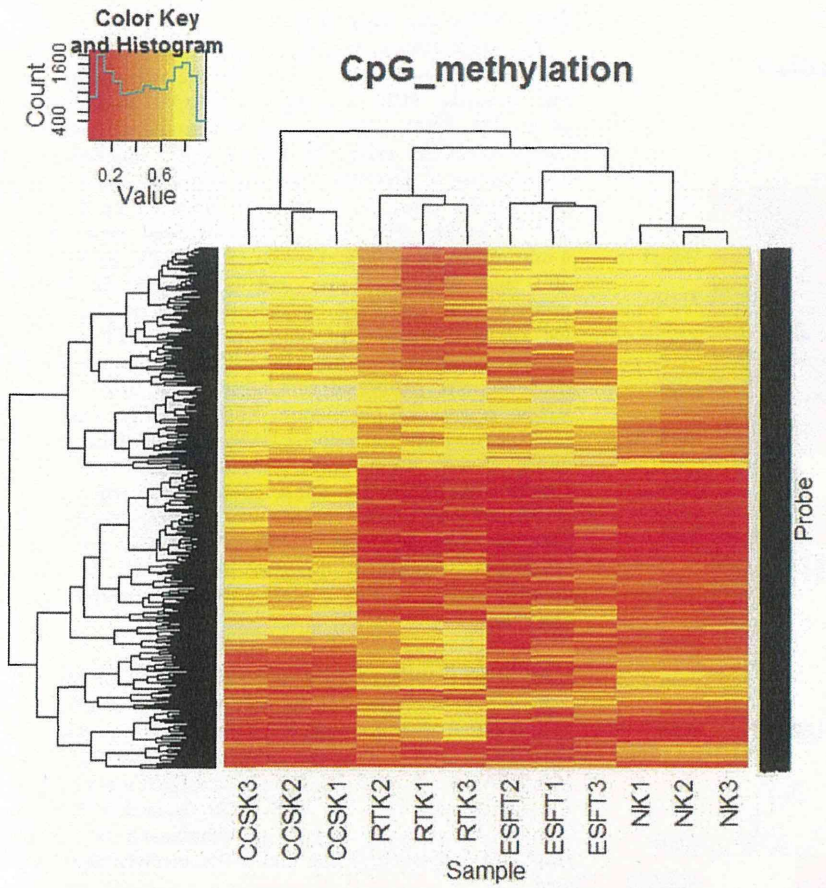


**Figure 1. Hierarchical cluster analysis of methylation value (β) in Infinium assay on pediatric tumors.** Two-way hierarchical cluster analysis of the methylation level of 1,494 probes (rows, equivalent to hyper- and hypomethylated genes shown in Table 2) and three cases for each of clear cell sarcoma of the kidney (CCSK), rhabdoid tumor of the kidney (RTK), the Ewing's sarcoma family of tumors (ESFT), and non-neoplastic kidney (NK) (columns) were performed using hclust in the R clustering package. The β-values ranged from 0 (unmethylated) to 1 (fully methylated) on a continuous scale.
doi:10.1371/journal.pone.0062233.g001

cells in each sample. The pathologic images of the disease tissues were presented in Figure S1. Genomic DNA was extracted from above evaluated fresh-frozen tissues using the illustra tissue & cells genomicPrep Mini Spin kit (GE Healthcare Bio-Sciences UK Ltd, Chalfont, UK) according to the manufacturer's instructions. The quantity of DNA was assessed by Quant-iT Pico-Green dsDNA Reagent and Kits (Life Technologies Corporation, Carlsbad, CA, USA) and the quality was assessed by agarose gel electrophoresis.

**Table 3.** The number of specifically methylated genes compared with other each of tumors and non-neoplastic kidney.

| | Hypermethylation | Hypomethylation |
|---|---|---|
| CCSK | 270 genes | 28 genes |
| RTK | 65 genes | 155 genes |
| ESFT | 7 genes | 35 genes |

Hypermethylation: difference of average β-value >0.3. Hypomethylation: difference of average β-value<−0.3.
doi:10.1371/journal.pone.0062233.t003

## Bisulfite Conversion

Starting from 1 μg of genomic DNA, bisulfite conversion of genomic DNA was performed using the Epitect Bisulfite kit (QIAGEN Inc., Valencia, CA, USA) and EZ DNA Methylation Kit (Zymo Research, Irvine, CA, USA) for the Illumina Infinium Methylation Assay and SEQUENOM MassARRAY, respectively, according to the manufacturer's protocol.

## Infinium Methylation Assay

Illumina Infinium HumanMethylation27 (Illumina, Inc., San Diego, CA, USA), containing the 27,578 CpG sites, spanning 14,495 genes, was used for methylation analysis. The bisulfite converted DNA was processed on the chip according to the Illumina protocol. The BeadChips were scanned using iScan system. Our data of Infinium assay have been deposited on Gene Expression Omnibus (GEO) database at the National Center for Biotechnology Information (NCBI, http://www.ncbi.nlm.nih.gov/geo/, series accession number GSE44847). The β-value and the detection p-value for each locus were calculated using GenomeStudio v2010.1. β-value, a ratio of methylated probe signal intensity to sum of methylated and unmethylated probe signal intensities, was used to estimate the methylation

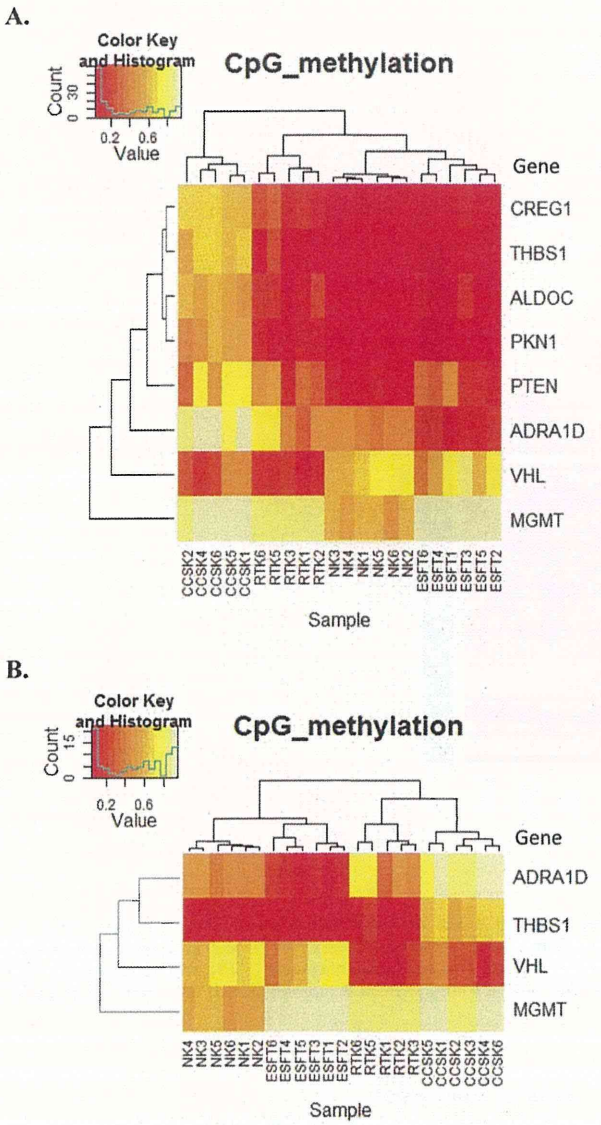


**Figure 2. Hierarchical cluster analysis of methylation level of CpG analyzed by MassARRAY.** (A) Based on the results indicated in Figure 1, 8 genes were selected as described in the text and analyzed by MassARRAY. Two-way hierarchical cluster analysis was performed using the CpG methylation average of all CpG that have passed QC from each gene. Two cases (RTK4 and CCSK3) showed failed analysis of some CpG sites, and were excluded from hierarchical analysis. (B) Four genes were further selected, and cluster analysis using the methylation average was performed as in (A). CCSK3 was successfully analyzed in all four genes, and included in this analysis.
doi:10.1371/journal.pone.0062233.g002

level of the target locus. Detection p-value is computed from the background model characterizing the chance that the target sequence signal was distinguishable from negative controls. The obtained data were filtered by exclusion of the probes with a detection p-value>0.05 from all probes and SD>0.2 within each entity. The numbers of the detected CpG sites for each sample and filtering process were shown in Table S1. As a result, 23,700 probes (13,385 genes) remained.

## EPITYPER Assay (MassARRAY)

The SEQUENOM EpiTYPER assay was performed according to the protocol recommended by the manufacturer. Using the Complete PCR Reagent Set (SEQUENOM Inc., San Diego, CA, USA), target regions were amplified from bisulfite-converted DNAs using the primer pairs containing a T7-promoter tag to allow further *in vitro* transcription. The primers used in this study (Table 1) were designed by EpiDesigner (SEQUENOM). The cycle conditions used were: 95°c for 4 min, 45 cycles of 95°C for 20 s, 56°C (65°C for *CREG1*) for 30 s. and, 95°C for 1 min, and 72°C for 3 min. The PCR products were confirmed by agarose gel electrophoresis. After the dephosphorylation of unincorporated dNTPs by shrimp alkaline phosphatase (SAP) (SEQUENOM), transcription and digestion were performed simultaneously at 37°C for 3 h by RNase A and T7 polymerase (SEQUENOM). The cleavage reactants were purified with CLEAN resin (SEQUENOME) and dispensed onto silicon chips preloaded with matrix (Spectro-CHIPS, SEQUENOM). Mass spectra were collected using a MassARRAY mass spectrometer (Bruker-Sequenom) and analyzed using proprietary peak picking and signal-to-noise calculations (Sequenom Epityper v1.0.5). In MassARRAY analysis, initially, quality control (QC) was performed in each CpG site.

## Combined Bisulfite Restriction Analysis (COBRA)

Bisulfite PCR products of *THBS1* produced as described above were digested with the methylation-sensitive restriction enzyme HpyCH4IV (5′-ACGT-3′) (New England Biolabs, NEB, Ipswich, MA, USA) for 12 h at 37°C The digested DNA was separated on 2% agarose gels in 0.5× TBE buffer, stained with ethidium bromide, and visualized on a UV transilluminator. As a control of HpyCH4IV digestion, 0, 50, and 100% methylated DNA were used.

## Statistical Analysis

Two-way hierarchical cluster analyses of Infinium assay and MassARRAY were performed using hclust in the R clustering package with Euclidean metric and complete linkage for statistical computing.

## Results

DNA methylation profiling of 3 each of CCSK, RTK, ESFT and NK, 12 samples in total, were performed using Infinium HumanMethylation27. First, we analyzed the general methylation status of each tumor group by defining hyper- and hypomethylated CpG sites in each tumor group as those with average β-value differences of >0.3 and <−0.3 compared to NK, respectively. The numbers of selected hyper- and hypomethylated CpG probes in each tumor are listed in Table 2. Among them, the number of selected hypermethylated CpG probes mapped on the CpG island in CCSK, RTK, and ESFT were 490, 130, and 66, respectively, while those of hypomethylated non-CpG probes were 117, 320, and 136, respectively (Table 2).

To test whether the tumors can be distinguished by the methylation level, we performed two-way hierarchical cluster analysis of methylation patterns using hyper- and hypomethylated sites (1,494 probes; equivalent to 1,281 genes selected in Table 2). As shown in Figure 1, each case in the same tumor was clustered in the same group, indicating the tumor-type-dependent methylation pattern of the selected probes.

To further select marker genes for methylation-based tumor-type classification, we defined tumor-specific differentially meth-

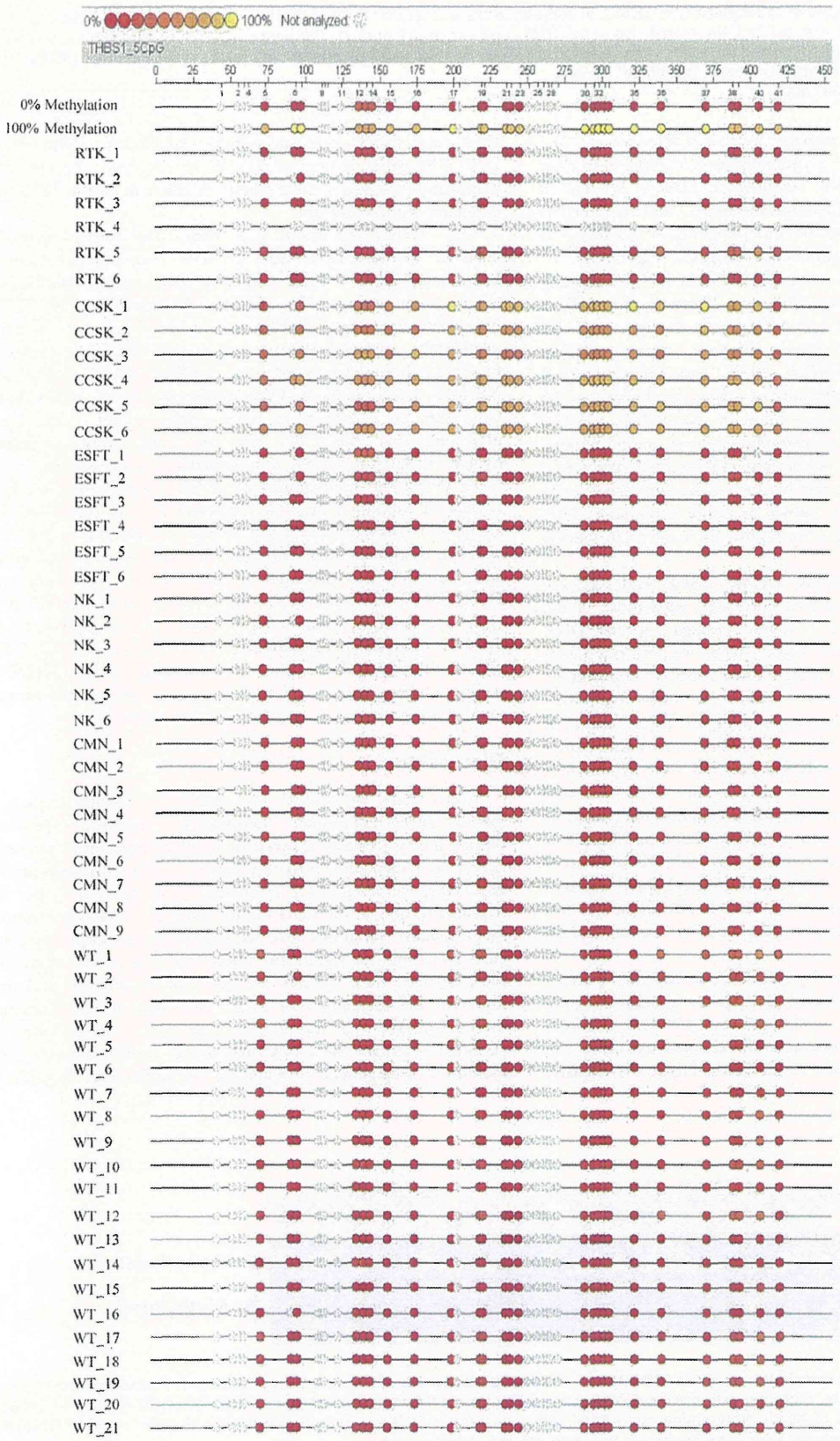
0%
100%
Not analyzed
THBS1_5CpG
0 25 50 75 100 125 150 175 200 225 250 275 300 325 350 375 400 425 450
0% Methylation
100% Methylation
RTK_1
RTK_2
RTK_3
RTK_4
RTK_5
RTK_6
CCSK_1
CCSK_2
CCSK_3
CCSK_4
CCSK_5
CCSK_6
ESFT_1
ESFT_2
ESFT_3
ESFT_4
ESFT_5
ESFT_6
NK_1
NK_2
NK_3
NK_4
NK_5
NK_6
CMN_1
CMN_2
CMN_3
CMN_4
CMN_5
CMN_6
CMN_7
CMN_8
CMN_9
WT_1
WT_2
WT_3
WT_4
WT_5
WT_6
WT_7
WT_8
WT_9
WT_10
WT_11
WT_12
WT_13
WT_14
WT_15
WT_16
WT_17
WT_18
WT_19
WT_20
WT_21

**Figure 3. MassARRAY analysis of methylation in *THBS1*.** In addition to the 6 cases for each tumor group, 9 and 21 cases of CMN and Wilms' tumor (WT), respectively, were analyzed for DNA methylation of the *THBS1* CpG site, as in Figure 2A. Different colored of circles mark the position of CpG within the sequence (straight line) and the levels of methylation are shown in color (red, low methylation level; yellow, high methylation level). Gray circles represent the unanalyzed CpG sites. WT: Wilms' tumor.
doi:10.1371/journal.pone.0062233.g003

ylated genes as those with average β-value differences of >0.3 (hypermethylated) or <−0.3 (hypomethylated) compared to each of other tumor groups and NK. As shown in Table 3, 270 and 28 genes were identified as CCSK-specific hyper- and hypomethylated genes, respectively, while 65 and 155 genes were selected as RTK-specific hyper- and hypomethylated genes, respectively.

Employing MassARRAY, next we analyzed the surrounding CpG of some specific probes filtered in Table 2, in detail to validate the results of an Infinium assay and further search for candidate genes for a differential diagnostic marker of renal sarcomas. Genes *ALDOC*, *CREG1*, *PKN1*, and *Thrombospondin-1* (*THBS1*) were selected because of their tendency to be hypermethylated in CCSK by the Infinium assay, while *ADRA1D* was selected because of distinct methylation levels among tumors. *MGMT* and *PTEN* were selected because of hypermethylation in 3 tumors, while *VHL* was selected because of hypomethylation in CCSK and RTK. These are known as tumor suppressor genes and these methylation changes are reportedly involved in specific tumors. [17,18].

We analyzed 6 each of RTK, CCSK, ESFT, and NK, the results of MassARRAY were well correlated with those of the Infinium assay, and each type of tumor revealed a specific DNA methylation pattern (Figure S2). In fact, when we performed two-way hierarchic cluster analysis using the CpG methylation average derived from the results, the cases for each tumor type were successfully classified into the same group (Figure 2A). As shown in Figure 2A, *CREG1*, *ALDOC*, *THBS1*, and *PKN1* were hypermethylated in CCSK, whereas RTK, ESFT, and NK were hypomethylated at specific CpG loci, as analyzed by the Infinium assay. *PTEN* was hypomethylated in NK, while variably methylated in sarcoma cases. *ADRA1D* was also hypermethylated in CCSK but hypomethylated in ESFT in comparison with NK, whereas variably methylated in RTK. Although *VHL* was hypomethylated in CCSK and RTK, it was hypermethylated in NK (Figure S3 and Figure S4). *MGMT* was hypermethylated in tumor groups compared to NK.

To distinguish these tumors by the DNA methylation pattern more simply, we further selected four genes characteristically methylated among different tumor groups: *ADRA1D*, *MGMT*, *VHL*, and *THBS1*, and performed cluster analysis using the methylation average of 4 genes. As shown in Figure 2B, CCSK, RTK, and ESFT were successfully classified according to the DNA methylation pattern of these genes, suggesting that the DNA methylation analysis of these 4 genes is sufficient for the differential diagnosis of these tumors.

Since *THBS1* was found to be characteristically hypermethylated in CCSK (Figure 2B), we next examined whether the hypermethylation of *THBS1* alone can distinguish CCSK from other tumor groups. To confirm the specificity of *THBS1* hypermethylation in CCSK among pediatric renal tumors, we additionally analyzed Wilms' tumor and CMN. As shown in Figure 3, when we analyzed 6 each of RTK, CCSK, ESFT, and NK as well as 21 cases of Wilms' tumor and 9 cases of CMN, the CpG sites of *THBS1* were unmethylated in all of the cases, indicating that the CpG sites of *THBS1* are specifically hypermethylated in CCSK among pediatric renal tumors.

To detect the methylation of *THBS1* more easily, we have developed combined bisulfite restriction analysis (COBRA) and analyzed 21 cases of CCSK and 41 cases of Wilms' tumor, 6 cases of RTK, 9 cases of CMN, and 6 cases of NK. As shown in Figure 4 and Table 4, the digestion of bisulfite PCR products with HpyCH4IV clearly indicated that a CpG site of *THBS1* in all CCSK cases was hypermethylated. However, none of other tumor groups exhibited hypermethylation of the CpG site of *THBS1*. The results strongly indicate that hypermethylation of *THBS1* is a specific characteristic of CCSK among pediatric renal tumors, and could be utilized as diagnostic maker of this tumor.

## Discussion

In this study, we carried out a DNA methylation analysis to identify genes differentially methylated in a series of pediatric tumors and we clearly showed that different pediatric sarcomas occurring in the kidney possess a distinct DNA methylation profile. Especially, CCSK is more frequently hypermethylated, but less hypomethylated, at the CpG island, compared with other tumors. Since pediatric renal sarcomas have overlapping morphologic and clinical features, the significant differences in epigenetic characteristics between these tumors are of particular interest and may represent the distinction of their cell origin or developmental mechanism. We also showed that these tumors can definitely be classified based on the DNA methylation profile, indicating the usefulness of epigenetic profiling for the differential diagnosis of

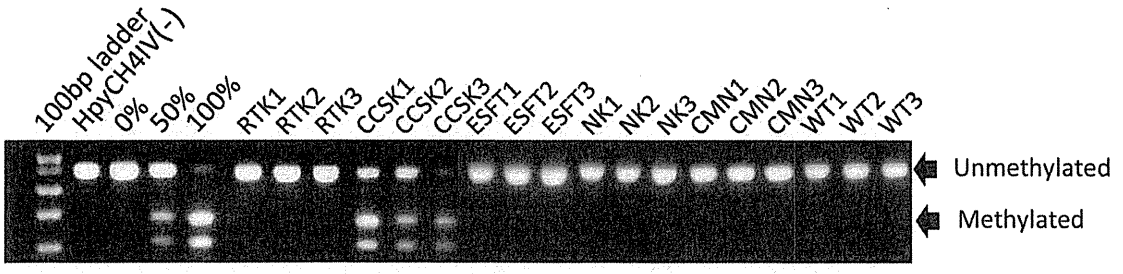


**Figure 4. Combined bisulfite restriction analysis (COBRA) of *THBS1* in pediatric renal tumors.** Using the same PCR products as in Figure 3, COBRA analysis was performed by digesting with the HpyCH4IV enzyme. The HpyCH4IV site is equivalent to CpG18 (chr15:37,660,642-37,660,645/hg18) in Figure 3. The positions of bands representing methylated and unmethylated DNA are indicated by arrows. As the control of HpyCH4IV digestion, 0, 50, and 100% methylated DNA were loaded on the same gel. WT: Wilms' tumor.
doi:10.1371/journal.pone.0062233.g004

**Table 4.** Frequency of *THBS1* methylation by COBRA.

| | Hypermethylated cases |
|---|---|
| RTK | 0/6 |
| CCSK | 21/21 |
| ESFT | 0/6 |
| CMN | 0/6 |
| Wilms | 0/41 |
| NK | 0/6 |

doi:10.1371/journal.pone.0062233.t004

pediatric renal sarcomas, and found that a combination of four genes is sufficient. Furthermore, the DNA methylation status of the *THBS1* CpG site detected by COBRA alone can distinguish CCSK cases from other pediatric renal tumors, including Wilms' tumor and CMN.

The pathological diagnoses of pediatric renal tumors are often supported by immunohistochemical and molecular genetic findings. For example, biallelic inactivation of *SMARCB1* as evidenced by negative immunohistochemical staining has high sensitivity and specificity for the diagnosis of RTK, and *ETV6-NTRK3* fusion is a marker for CMN of the cellular type. In the case of CCSK, however, it has neither immunohistochemical nor molecular genetic markers, while *YWHAE-FAM22* fusion was reported in only a minority [19]. Since *THBS1* hypermethylation is highly specific for CCSK, as we presented in this study, this finding should be useful for a molecular marker of this tumor. Especially, COBRA of the *THBS1* CpG site is highly accurate, reproducible, and can be performed without particular equipment, and, thus, it could be a candidate for routine examination for the differential diagnosis of CCSK from other pediatric renal tumors.

DNA methylation has been proposed as a diagnostic marker for certain cancers. For example, Goto reported that malignant mesothelioma could be differentiated from lung adenocarcinoma by methylation profiles [20], and Mahoney reported that embryonal and alveolar subtypes of rhabdomyosarcoma have a distinct DNA methylation profile [21]. In their cases, however, the methylation status of at least several genes was required for the differentiation of only two entities. In contrast, our findings showed that hypermethylation of a single locus of *THBS1* is sufficient for the differentiation of CCSK from other pediatric tumors and it could serve as a robust diagnostic marker for this tumor.

Hypermethylation of the *THBS1* CpG site has been observed in some tumors. For example, Guo et al. reported that the rate of methylation of *THBS1* was significantly higher in gastric cardia adenocarcinoma than that in the corresponding normal tissues and accompanied by reduction of its mRNA and protein expressions [22], and Guerrero et al. also reported that the hypermethylation of *THBS1* is associated with a poor prognosis in penile squamous cell carcinoma [23]. In both cases, the hypermethylation of *THBS1* has been suggested to be correlated with the pathogenesis.

THBS1 is a member of the thrombospondin family, and is known for putative antiangiogenic factor [24,25]. By employing a knockout mouse model, several studies have shown that the absence of *THBS1* leads to increased vascularization and THBS1 protein inhibits tumor progression in several ways, including direct effects on cellular growth and apoptosis in the stromal compartment [26–29]. Since CCSK is known to be rich in a fine vascular network, it is reasonable to presume that hypermethylation of the *THBS1* CpG site is involved in the pathogenesis of CCSK. However, we observed no significant correlations between the methylation status and expression of THBS1 by realtime RT-PCR and immunohistochemistry (data not shown). This is possibly due to hypermethylated CpG sites of *THBS1* in CCSK that we identified as not being responsible for *THBS1* expression, and other CpG sites are related to the regulation of *THBS1* expression. In fact, other CpG probes (cg19570574: chr15: 37660116–37660117/hg18, cg04051458: chr15: 37660352–37660353/hg18) in the upstream region of the *THBS1* transcription start site were hypomethylated in CCSK based on our assay. Another possibility is that THBS1 is expressed in a limited period during tumorigenesis. Further studies to elucidate the biological significance of CCSK hypermethylation are now underway.

In conclusion, pediatric renal sarcomas possess a distinct DNA methylation profile in a tumor-type-specific manner. The DNA methylation status of the *THBS1* CpG site detected by COBRA alone is sufficient for the distinction of CCSK from other pediatric renal tumors. Although further analysis to elucidate the biological importance of the differential DNA methylation of each tumor is required, our observation should shed light on the significance of the epigenetic diversity of pediatric renal tumors on their biological features and mechanism of pathogenesis.

## Supporting Information

**Figure S1 Images of frozen tissue sample by H.E. staining.** Frozen tumor tissues were embedded in OCT-compound and sectioned in 6 μm, stained with H.E. The proportion of viable tumor tissue was evaluated under light microscope.
(TIF)

**Figure S2 Correlation of the methylation values between Infinium assay and MassARRAY.** In cases of *THBS1* and *CREG1*, methylation values of same CpG site measured by MassARRAY (average of 6 samples) and Infinium BeadChip Assays (average of 3 samples) were indicated in the scattergrams and values of coefficient of determination ($R^2$) were calculated. In case of *VHL*, two probe sites were shown. Since each site of *VHL* could not be discriminated from the neighbouring site by MassARRAY, the methylation value was obtained as an average of two sites. Coefficient of determination between the values obtained by two methods was larger than 0.99 in each case. Methylation levels of the equivalent CpG sites were correlated between Infinium assay and MassARRAY.
(TIF)

**Figure S3 MassARRAY analysis of *VHL* in pediatric renal tumors.** MassARRAY analysis of the *VHL* was carried out in 6 each of RTK, CCSK, ESFT, NK. Different colored of circles mark the position of CpG within the sequence (straight line) and the levels of methylation are shown in color (red, low methylation level; yellow, high methylation level). Gray circles represent the unanalyzed CpG sites. CpG5 and CpG13 are equivalent to Infinium assay probes.
(TIF)

**Figure S4 Combined bisulfite restriction analysis (COBRA) of *VHL* in pediatric renal tumors.** Bisulfite PCR amplification of *VHL* was carried out by using same primer for MassArray. COBRA analysis was performed by digesting with the TaqI restriction enzyme. The TaqI site is equivalent to CpG3 in MassARRAY analysis. The site of genome sequence is CCGA, which is converted to TaqI sequence (tCGA) by bisulfite reaction. PCR amplification of RTK4 was failed. The digested DNA was

separated on 2% agarose gels in 1×TAE buffer, stained with ethidium bromide, and visualized on a UV transilluminator. (TIF)

**Table S1** Numbers of probes filtered with p-value and SD. (DOCX)

## Acknowledgments

We thank Keiko Nakasato for technical assistance.

## References


1. Eble JN, Sauter G, Epstein JI, Sesterhenn IA (2004) World Health Organization Classification of Tumours: Pathology and Genetics of Tumours of the Urinary System and Male Genital Organs. Lyon: IARC Press. p48–61.
2. Rubin BP, Chen CJ, Morgan TW, Xiao S, Grier HE, et al. (1998) Congenital mesoblastic nephroma t(12;15) is associated with ETV6-NTRK3 gene fusion: cytogenetic and molecular relationship to congenital (infantile) fibrosarcoma. Am J Pathol. 153: 1451–1458.
3. Argani P, Perlman EJ, Breslow NE, Browning NG, Green DM, et al. (2000) Clear cell sarcoma of the kidney: a review of 351 cases from the National Wilms Tumor Study Group Pathology Center. Am J Surg Pathol 24: 4–18.
4. Versteege I, Sevenet N, Lange J, Rousseau-Merck MF, Ambros P, et al. (1998) Truncating mutations of hSNF5/INI1 in aggressive pediatric cancer. Nature 394: 203–206.
5. Biegel JA, Tan L, Zhang F, Wainwright L, Russo P, et al. (2002) Alterations of the hSNF5/INI1 gene in central nervous system atypical teratoid/rhabdoid tumors and renal and extrarenal rhabdoid tumors. Clin Cancer Res 8: 3461–3467.
6. Imbalzano AN, Jones SN (2005) Snf5 tumor suppressor couples chromatin remodeling, checkpoint control, and chromosomal stability. Cancer Cell 7: 294–295.
7. Beckwith JB (1994) Renal neoplasms of childhood. 2nd ed. In: Sternberg SS, editor. Diagnostic surgical pathology. New York: Raven Press. 1741–1766.
8. Schuster AE, Schneider DT, Fritsch MK, Grundy P, Perlman EJ (2003) Genetic and genetic expression analyses of clear cell sarcoma of the kidney. Lab Invest 83: 1293–1299.
9. Baylin SB, Belinsky SA, Herman JG (2000) Aberrant methylation of gene promoters in cancer–concepts, misconcepts, and promise. J Natl Cancer Inst 92: 1460–1461.
10. Feinberg AP, Tycko B (2004) The history of cancer epigenetics. Nat Rev Cancer 4: 143–153.
11. Esteller M. (2002) CpG island hypermethylation and tumor suppressor genes: a booming present, a brighter future. Oncogene 21: 5427–5440.
12. Herman JG, Baylin SB (2003) Gene silencing in cancer in association with promoter hypermethylation. N Engl J Med 349: 2042–2054.
13. Anglesio MS, Evdokimova V, Melnyk N, Zhang L, Fernandez CV, et al. (2004) Differential expression of a novel ankyrin containing E3 ubiquitin-protein ligase, Hace1, in sporadic Wilms' tumor versus normal kidney. Hum Mol Genet. 13(18): 2061–2074.
14. Haruta M, Matsumoto Y, Izumi H, Watanabe N, Fukuzawa M, et al. (2008) Combined BuR1 protein down-regulation and RASSF1A hypermethylation in Wilms tumors with diverse cytogenetic change. Mol Carcinog. 47(9): 660–666.
15. Szemes M, Dallosso AR, Melegh Z, Curry T, Li Y, et al. (2013) Control of epigenetic states by WT1 via regulation of de novo DNA methyltransferase 3A. Hum Mol Genet. 22(1): 74–83.
16. Chilukamarri L, Hancock AL, Malik S, Zabkiewicz J, Baker JA, et al. (2007) Hypomethylation and aberrant expression of the glioma pathogenesis-related 1 gene in Wilms tumors. Neoplasia. (11): 970–978.
17. Esteller M, Herman JG (2004) Generating mutations but providing chemosensitivity: the role of O6-methylguanine DNA methyltransferase in human cancer. Oncogene. 23(1): 1–8.
18. Yu J, Ni M, Xu J, Zhang H, Gao B, et al. (2002) Methylation profiling of twenty promoter-CpG islands of genes which may contribute to hepatocellular carcinogenesis. J.BMC Cancer. 2: 29.
19. O'Meara E, Stack D, Lee CH, Garvin AJ, Morris T, et al. (2012) Characterization of the chromosomal translocation t(10;17)(q22;p13) in clear cell sarcoma of kidney. J Pathol. 227(1): 72–80.
20. Goto Y, Shinjo K, Kondo Y, Shen L, Toyota M, et al. (2009) Epigenetic profiles distinguish malignant pleural mesothelioma from lung adenocarcinoma. Cancer Res. 69(23): 9073–9082.
21. Mahoney SE, Yao Z, Keyes CC, Tapscott SJ, Diede SJ (2012) Genome-wide DNA methylation studies suggest distinct DNA methylation patterns in pediatric embryonal and alveolar rhabdomyosarcomas. Epigenetics 7(4): 400–408.
22. Guo W, Dong Z, He M, Guo Y, Guo J, et al. (2010) Aberrant methylation of thrombospondin-1 and its association with reduced expression in gastric cardia adenocarcinoma. J Biomed Biotechnol 721485 Epub 2010 Mar 15.
23. Guerrero D, Guarch R, Ojer A, Casas JM, Ropero S, et al.(2008)Hypermethy-)Hypermethylation of the thrombospondin-1 gene is associated with poor prognosis in penile squamous cell carcinoma. BJU Int. 102: 747–755.
24. Lawler J (2002) Thrombospondin-1 as an endogenous inhibitor of angiogenesis and tumor growth. J Cell Mol Med 6: 1–12.
25. Folkman J (2004) Endogenous angiogenesis inhibitors. APMIS 112: 496–507.
26. Greenaway J, Lawler J, Moorehead R, Bornstein P, Lamarre J, et al.(2007) Thrombospondin-1 inhibits VEGF levels in the ovary directly by binding and internalization via the low density lipoprotein receptor-related protein-1 (LRP-1). J Cell Physiol 210: 807–818.
27. Wang S, Wu Z, Sorenson CM, Lawler J, Sheibani N (2003) Thrombospondin-1-deficient mice exhibit increased vascular density during retinal vascular development and are less sensitive to hyperoxia-mediated vessel obliteration. Dev Dyn 228: 630–642.
28. Lawler J, Miao WM, Duquette M, Bouck N, Bronson RT, et al. (2001) Thrombospondin-1 gene expression affects survival and tumor spectrum of p53-deficient mice. Am J Pathol 159: 1949–1956.
29. Sund M, Hamano Y, Sugimoto H, Sudhakar A, Soubasakos M, et al. (2005) Function of endogenous inhibitors of angiogenesis as endothelium-specific tumor suppressors. Proc Natl Acad Sci USA 102: 2934–2939.


## Author Contributions

Conceived and designed the experiments: HU HO NK. Performed the experiments: HU HO SA KN. Analyzed the data: HU HO. Contributed reagents/materials/analysis tools: HO JF JH MF KN KH. Wrote the paper: HU HO KK NK.